Inorganic polyphosphate abets silencing of a sub-telomeric gene cluster in fission yeast

Ana M. Sanchez[1,2§], Angad Garg[1], Beate Schwer[3], Stewart Shuman[1]

[1]Molecular Biology, Memorial Sloan Kettering Cancer Center, New York, New York, United States

[2]Gerstner Sloan Kettering Graduate School of Biomedical Sciences, New York, New York, United States

[3]Microbiology and Immunology, Weill Cornell Medicine, New York, New York, United States

[§]To whom correspondence should be addressed: sanchea6@mskcc.org

Abstract

Inorganic polyphosphate is a ubiquitous polymer with myriad roles in cell and organismal physiology. Whereas there is evidence for nuclear polyphosphate, its impact on transcriptional regulation in eukaryotes is unkown. Transcriptional profiling of fission yeast cells lacking polyphosphate (via deletion of the catalytic subunit Vtc4 of the Vtc4/Vtc2 polyphosphate polymerase complex) elicited de-repression of four protein-coding genes located within the right sub-telomeric arm of chromosome I that is known to be transcriptionally silenced by the TORC2 complex. These genes were equally de-repressed in *vtc2Δ* cells and in cells expressing polymerase-dead Vtc4, signifying that polyphosphate synthesis is required for repression of these sub-telomeric genes.
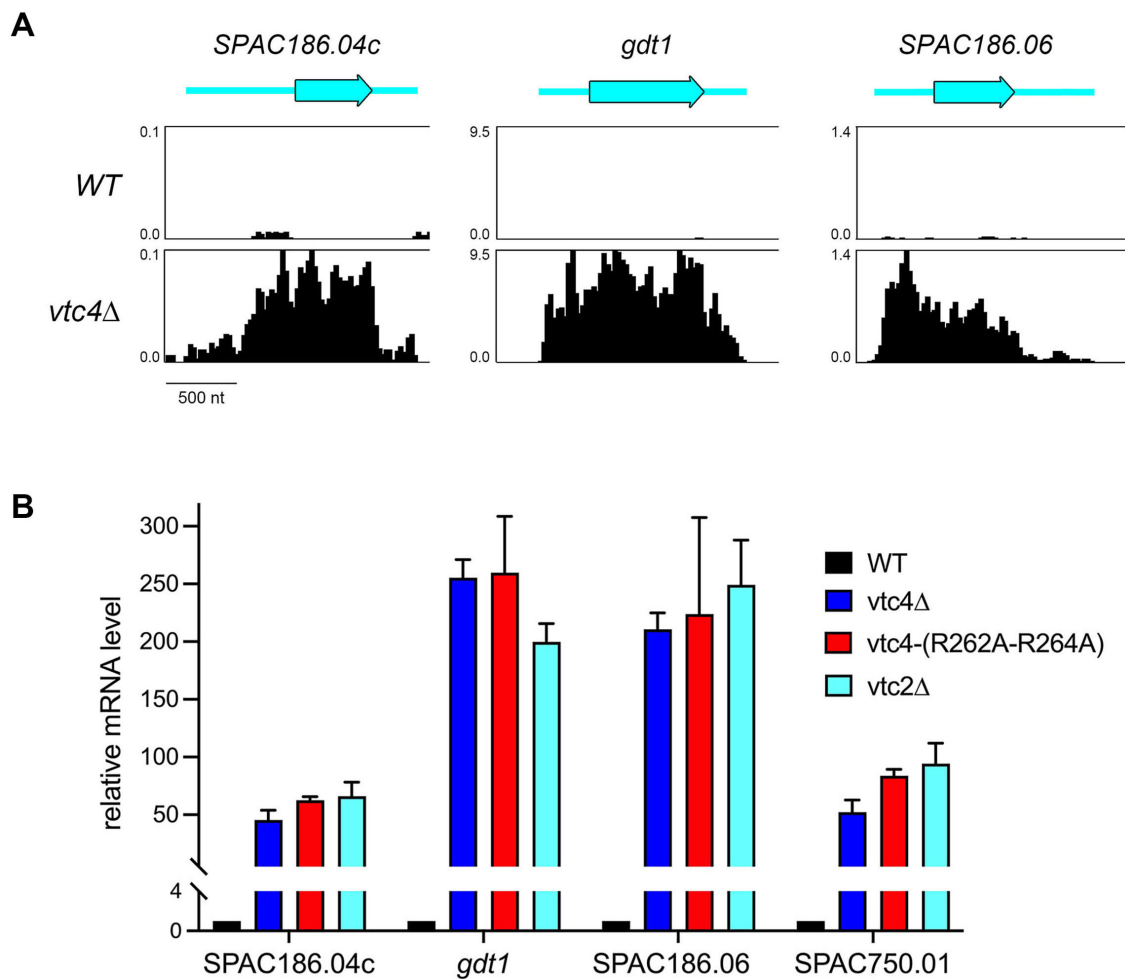
Figure 1. Polyphosphate synthesis by Vtc4 polyP polymerase is required for silencing sub-telomeric genes:

(A) Strand-specific RNA-seq read densities (counts/base/million, averaged in a 25-nt window) of the indicated strains are plotted on the y-axis as a function of position across the loci (x-axis). The read densities were determined from cumulative counts of all three RNA-seq replicates for each *S. pombe* strain. The y-axis scale for each track is indicated. The common x-axis scale is shown on the bottom left. The individual ORFs are labeled and shown to scale as black-outlined thick cyan arrows. The 5' and 3' UTRs are depicted as thin cyan bars. **(B)** The analysis of mRNA levels for *SPAC186.04c*, *gdt1*, *SPAC186.06*, *SPAC750.01* in *WT*, *vtc4Δ*, *vtc4-R262A,R264A*, and *vtc2Δ* yeast strains was performed as described in Methods. The level of each transcript was normalized to that of *act1* for the same RNA sample. The bar graph shows relative change in mRNA levels in *vtc4Δ*, *vtc4-R262A,R264A*, and *vtc2Δ* relative to the wild-type control (defined as 1.0). Each datum in the graph is the average value of RT-qPCR analyses of RNA from three independent yeast cultures; the error bars denote SEM.

Description

Inorganic polyphosphate (polyP) is an anionic linear polymer of heterogeneous length found in taxa from all phylogenetic domains. PolyP levels and polymer chain length are determined by a dynamic balance between synthesis by polyP kinase or polyP polymerase enzymes and catabolism by exopolyphosphatase or endopolyphosphatase enzymes and may fluctuate in response to stress or developmental and environmental cues (Kornberg et al. 1999). PolyP plays diverse roles in physiology: as an energy source; a phosphate reservoir during phosphate starvation; a metal chelator; a modulator of blood clotting and fibrinolysis; a post-translation protein modification (lysine polyphosphorylation); a microbial virulence factor; a signaling molecule (Kornberg et al. 1999, Azevedo et al. 2014, Gray et al. 2014, Azevedo et al. 2015, Baker et al. 2018, Bowlin & Gray 2021).

PolyP is especially abundant in yeast cells, e.g., the intracellular concentration of inorganic polyphosphate in budding yeast grown in phosphate-replete medium is 230 mM (with respect to phosphate residues) as compared to 23 mM for orthophosphate (Auesukaree et al. 2004). Yeast polyP is produced by a heterotrimeric membrane-associated VTC complex that synthesizes polyP and simultaneously imports the polyP into the yeast vacuole (Gerasimaite & Mayer 2014, Hothorn et al. 2009, Gerasimaite et al. 2014). Budding yeast has two VTC complexes: the VTC associated with the vacuole consists of Vtc4, Vtc3, and Vtc1 proteins; the VTC associated with the endoplasmic reticulum and nuclear envelope comprises Vtc4, Vtc2, and Vtc1 subunits (Gerasimaite & Mayer 2014, Gerasimaite et al. 2014). Fission yeast has a single heterotrimeric VTC complex that includes a Vtc2 subunit.

Vtc4 is the catalytic subunit of the polyP polymerase; it consists of a cytoplasm-facing N-terminal SPX domain, a central polymerase domain, and a C-terminal membrane anchor domain (Gerasimaite & Mayer 2014). The SPX domain binds and senses the inositol pyrophosphate signaling molecules IP_7 and IP_8 that stimulate polyP synthesis by VTC (Wild et al. 2016, Gerasimaite et al. 2017, Pascual-Ortiz et al. 2021, Schwer et al. 2022). The Vtc4 polymerase domain, which catalyzes manganese-dependent transfer of an NTP γ-phosphate to an inorganic pyrophosphate or phosphate primer (Hothorn et al. 2009), is a member of the triphosphate tunnel metalloenzyme (TTM) family (Lima et al. 1999, Martinez at al. 2015). Vtc2 and Vtc3 are paralogs homologous to Vtc4, but their TTM domains are catalytically inactive.

In budding yeast, vacuolar polyphosphate comprises ~80% of the total polyP content. There exists a pool of nuclear polyP (dependent on Vtc4) that persists in yeast cells engineered so that the intra-vacuolar pool of polyP is depleted (Azevedo & Saiardi 2014, Azevedo et al. 2020). These findings raise the question of whether polyP plays a role in nuclear transactions, especially in gene expression. To our knowledge, there is scant information on whether physiological levels of polyP impact transcriptional regulation in eukarya. To rectify this knowledge gap, we performed transcriptional profiling of fission yeast *vtc4Δ* cells that have no detectable intracellular polyP (Pascual-Ortiz et al. 2021, Schwer et al. 2022).

cDNAs obtained from three biological replicates, using poly(A)$^+$ RNA from wild-type and *vtc4Δ* cells grown to mid-log phase in YES medium at 30˚C, were sequenced. Read densities for individual genes were highly reproducible between biological replicates (Pearson coefficients of 0.98 to 0.99). A cutoff of ±2-fold change in normalized transcript read level and an adjusted p-value of ≤0.05 were the criteria applied to derive a list of differentially expressed annotated loci in the *vtc4Δ* mutant versus the wild-type control. We then focused on differentially expressed genes with average normalized read counts ≥100 in either strain to initially exclude transcripts that were expressed at very low levels in vegetative cells. We thereby identified 36 protein-coding genes that were down-regulated and 6 protein-coding genes that were up-regulated by these criteria in *vtc4Δ* cells (Table 1). All 36 genes in the former set were down-regulated modestly, between 2-fold and 4-fold *vis-à-vis* wild-type. Among the *vtc4Δ* down-regulated genes were those encoding enzymes of glycolysis and sugar metabolism: enolase (Eno102 and Eno101), glyceraldehyde-3-phosphate dehydrogenase Gpd3, glucose dehydrogenase Gcd1, transaldolase Tal1, and phosphoketolase SPBC24C6.09c. Among the up-regulated gene set, 3 coding transcripts were very strongly up-regulated: *gdt1(SPAC186.05c)* by 111-fold; *SPAC186.06* by 52-fold; and *SPAC750.01* by 46-fold (Table 1). The 3 other transcripts were increased by only 2-fold in *vtc4Δ* cells. At this stage, the RNA-seq data suggested that the presence of polyP in wild-type cells

might strongly repress the expression of a very narrow set of fission yeast transcripts. Therefore, we reset the cut-off criteria at a four-fold change in *vtc4Δ* versus wild-type and imposed no minimum threshold for read counts. This revealed one additional gene upregulated in *vtc4Δ* cells: *SPAC186.04c* by 46-fold (Table 1).

The protein products of the four *vtc4Δ* up-regulated genes appear unconnected functionally: *gdt1* encodes a Golgi calcium and manganese transporter (Colinet et al. 2016); SPAC186.06 is a yeast homolog of phenazine biosynthesis enzyme PhzF (Liger et al. 2005); SPAC750.01 is a putative NADP-dependent aldo/keto reductase; SPAC186.04c is of unknown function. Their unifying property is that they are located physically within a sub-telomeric region of the right arm of chromosome I that is known to be transcriptionally silenced during unstressed vegetative growth (Cohen et al. 2018). The RNA-seq read counts across the cluster of adjacent *SPAC186.04c*, *gdt1*, and *SPAC186.06* genes in wild-type and *vtc4Δ* cells show that the up-regulated RNA spans the entire predicted ORF and flanking UTRs, the dimensions of which can be surmised from the *vtc4Δ* RNA-seq profiles (Fig. 1A).

Weisman and colleagues have established that: (i) the fission yeast TORC2 complex (containing the Tor1 protein kinase) and its downstream effector protein kinase Gad8 are present in the nucleus and bound to chromatin (Cohen et al. 2016, Laribee & Weisman 2020); and (ii) TORC2 and Gad8 function to silence the expression of a set of 7 sub-telomeric genes on chromosomes I and II (Cohen et al. 2018) that, not coincidentally, includes all four of the genes up-regulated by *vtc4Δ*. These sub-telomeric genes are strongly up-regulated in *tor1Δ* and *gad8Δ* cells; they are also de-repressed in *ste20Δ* and *ryh1Δ* cells that respectively lack the TORC2 subunit Ste20 and the Ryh1 GTPase that activates TORC (Cohen et al. 2018). The de-repression of the sub-telomeric loci in *tor1Δ* and *gad8Δ* cells correlates with: (i) loss of the repressive H3K9Me2 chromatin mark over the loci; (ii) gain of the H3K4me3 and H4K16Ac activation marks; and (iii) increased locus occupancy by Pol2 (Cohen et al. 2018). Further studies showed that increased expression of the *gdt1(SPAC186.05c)*, *SPAC186.04c*, and *SPAC186.06* genes in *tor1Δ* cells depends on Pol2 transcription activators Leo1, Med1, and Gcn5 (Cohen et al. 2022). Our transcriptional profiling implicates the VTC complex as a collaborator in TORC2 silencing of the sub-telomeric four-gene cluster on chromosome I.

A salient question is whether the transcriptional impact of *vtc4Δ* on sub-telomeric gene silencing is a consequence of the absence of polyP or the interdiction of a hypothetical function of Vtc4 other than polyP synthesis. If the VTC complex is necessary for silencing, then we would expect that deletion of the Vtc2 subunit would phenocopy *vtc4Δ*. The requirement for catalysis by Vtc4 can be interrogated via a polymerase active site mutation R262A,R264A in Vtc4 that eliminates polyP in fission yeast (Schwer et al. 2022). To gauge expression of the four sub-telomeric genes in wild-type, *vtc4Δ*, *vtc2Δ*, and *vtc4-R262A,R264A* genetic backgrounds, we performed transcript-specific RT-qPCR of total RNA isolated from these four strains. RT-qPCR analysis of *act1* mRNA was included as a control. The sub-telomeric transcript levels were normalized to *act1* for each sample and are plotted in Fig. 1B, such that the changes in transcript levels in the *vtc* mutants are normalized to transcript levels of wild-type cells. The findings were as follows: (i) RT-qPCR affirmed that *gdt1*, *SPAC186.04c*, *SPAC186.06,*and *SPAC750.01* were strongly de-repressed in *vtc4Δ* cells; (ii) similar extents of de-repression were observed in *vtc2Δ* and *vtc4-R262A,R264A* cells, signifying that polyP synthesis by the VTC complex is required for silencing of these sub-telomeric genes.

The results presented here anent the de-repression of a cluster of normally silenced sub-telomeric genes in fission yeast when polyP synthesis is interdicted genetically resonate with the recent discovery by Jakob and colleagues that deletion of polyP kinase in *E. coli* elicits up-regulation of transcription of normally silenced chromosomal regions containing mobile genetic elements and prophages (Beaufay et al. 2021). Their experiments indicate that polyP collaborates with bacterial Hfq and AT-rich DNA to nucleate phase-separated condensates. They propose that polyP drives the formation of localized heterochromatin in bacteria (Beaufay et al. 2021).

Analogous genetic studies of polyP physiology in mammalian cells are not feasible at present, because the mammalian enzyme(s) responsible for polyP synthesis are not known (Desfougères et al. 2020). A surrogate approach has been to overproduce polyP in mammalian cells via ectopic expression of bacterial polyP kinase and document the effects thereof. When this maneuver was applied to human cells, it was found that: (i) high levels of long-chain polyP accumulated in multiple intracellular compartments; and (ii) 313 genes were down-regulated and 47 genes were upregulated in polyP kinase-expressing cells, by the criterion of a statistically significant 25% difference versus non-expressing cells (Bondy-Chorney et al. 2020). If a ≥2-fold difference cut-off is applied, then 102 genes were down-regulated and 8 genes were upregulated. There are caveats to this approach when it comes to inferences about polyP function. To wit: (i) the levels of polyP achieved are excessive, hence non-physiological; (ii) the polyP may localize to intracellular sites where it is not normally present; and (iii) the polyP that does accumulate is skewed toward very long chains. Indeed, studies in budding yeast indicate that forced accumulation of non-physiological levels of polyphosphate outside the vacuole and membrane compartments, achieved via expression of a bacterial

polyP kinase, is *per se* cytotoxic (Gerasimaite et al. 2014). Coupling of VTC-mediated polyphosphate polymerase activity to vacuolar or intramembrane import of the polyphosphate product is a means to avoid such toxicity (Gerasimaite et al. 2014).

The present data instate a role for fission yeast polyP in localized gene silencing, presumably as a participant in the TORC2 pathway of sub-telomeric silencing discovered by the Weisman lab. Based on available knowledge, we can speculate on at least two ways in which polyP may accomplish this. First, polyP can exert effects on cell physiology via non-enzymatic lysine polyphosphorylation of target proteins in vivo, including nuclear proteins such as DNA topoisomerase I, Nsr1, and ribosome biogenesis factors (Azevedo et al. 2015, Bentley-DeSousa et al. 2018, Azevedo et al. 2020). Indeed, among the validated targets of in vivo lysine polyphosphorylation in budding yeast are several proteins involved in chromatin biology: histone H2AZ chaperone Chz1, histone acetyltransferase complex subunit Eaf7, nucleosome assembly factor Hpc2 (Bentley-DeSousa et al. 2018). If lysine polyphosphorylation of nuclear proteins that establish or maintain silenced chromatin over the fission yeast chromosome I sub-telomeric cluster is important for their activity, then ablation of polyP synthesis would elicit the observed de-repression. Given that the TORC2 pathway is necessary for silencing the cluster in fission yeast, it is possible TORC2 or pathway components acting downstream are subject to lysine polyphosphorylation. Second, taking a cue from the recent studies in *E. coli* (Beaufay et al. 2021), polyP might promote the assembly of repressive factors at the affected loci, by providing a scaffold for their recruitment to form a higher order polyP–protein–DNA assembly, with or without accompanying phase separation. Other models or mechanisms for polyP-mediated silencing are in no way off the table. In conclusion, the initial findings here provide an impetus for further interrogation of polyP function in fungal gene expression.

Table 1. List of protein-coding genes that were dysregulated at least two-fold in *vtc4Δ* cells compared to the wild-type strain. The log2 fold changes are shown.

Systematic ID	Gene	Product	log2 fold change
upregulated			
SPAC186.05c	gdt1	Golgi calcium and manganese antiporter	6.82
SPAC186.06		PhzF protein family	5.71
SPAC750.01		NADP-dependent aldo/keto reductase	5.52
SPAC186.04c		–	5.55
SPBPB10D8.03		pseudogene transporter	1.29
SPCC1223.13	cbf12	DNA-binding transcription factor	1.10
SPBC1711.15c		Schizosaccharomyces pombe specific protein	1.00
downregulated			
SPBC16E9.16c	lsd90	Lsd90 protein	-2.05
SPBC1289.14		adducin	-1.88
SPCC794.04c		amino acid transmembrane transporter	-1.80
SPACUNK4.17		NAD binding dehydrogenase	-1.76
SPBPB21E7.01c	eno102	enolase	-1.63

SPBC336.08	spc24	NMS complex subunit	-1.62
SPBC16A3.08c	oga1	Stm1 homolog	-1.61
SPAC15E1.02c		DUF1761 family protein	-1.59
SPBC354.12	gpd3	glyceraldehyde 3-phosphate dehydrogenase	-1.57
SPAC27D7.03c	mei2	RNA-binding protein involved in meiosis	-1.49
SPBC21C3.19	rtc3	SBDS family protein	-1.39
SPAP8A3.04c	hsp9	heat shock protein	-1.36
SPCC1235.14	ght5	high-affinity glucose/fructose:proton symporter	-1.32
SPAC637.03		DUF1774 family	-1.29
SPBC725.10	tsp0	mitochondrial outer membrane protein	-1.27
SPBC23G7.13c		urea transmembrane transporter	-1.27
SPAC13G7.02c	ssa1	Hsp70 family heat shock protein	-1.18
SPBC660.06	wwm2	WW domain containing protein	-1.18
SPCC794.09c	tef101	translation elongation factor EF-1 alpha	-1.17
SPAC23H3.15c	ddr48	DNA damage-responsive protein	-1.17
SPCC794.01c	gcd1	glucose dehydrogenase	-1.13
SPBPB8B6.04c	grt1	DNA-binding transcription factor	-1.09
SPCC737.04		UPF0300 family protein 6	-1.08
SPBC839.15c	tef103	translation elongation factor EF-1 alpha	-1.08
SPAC22A12.17c		short chain dehydrogenase	-1.07
SPAC26H5.09c		oxidoreductase in NADPH regeneration	-1.07
SPBC24C6.09c		phosphoketolase family protein	-1.07
SPAC23A1.10	tef102	translation elongation factor EF-1 alpha	-1.07
SPAC1039.09	isp5	amino acid transmembrane transporter	-1.05

SPCC338.12	pbi2	vaculoar proteinase B inhibitor	-1.04
SPBC1815.01	eno101	enolase	-1.04
SPBC29B5.02c	isp4	oligopeptide transmembrane transporter	-1.03
SPAC26F1.14c	aif1	mitochondrial oxidoreductase	-1.03
SPAC1805.10		Schizosaccharomyces specific protein	-1.03
SPAC186.01	pfl9	cell surface glycoprotein, flocculin	-1.00
SPCC1020.06c	tal1	transaldolase	-1.00

Methods

Transcriptome profiling by RNA-seq.

RNA was isolated from *S. pombe* wild-type and *vtc4Δ* cells that were grown in liquid YES medium at 30°C to an A_{600} of 0.5 to 0.6. Cells were harvested by centrifugation and total RNA was extracted via the hot phenol method. The integrity of total RNA was gauged with an Agilent Technologies 2100 Bioanalyzer. The Illumina TruSeq stranded mRNA sample preparation kit was used to purify poly(A)$^+$ RNA from 500 ng of total RNA and to carry out the subsequent steps of poly(A)$^+$ RNA fragmentation, strand-specific cDNA synthesis, indexing, and amplification. Indexed libraries were normalized and pooled for paired-end sequencing performed by using an Illumina NovaSeq 6000-S1 flow cell. FASTQ files bearing paired-end reads of length 51 bases (total paired reads of 19.1 million to 27.5 million per biological replicate) were mapped to the *S. pombe* genome (Pombase) using HISAT2-2.1.0 with default parameters (Kim et al. 2015). Mapped reads comprised 93% to 96% of the total reads per replicate. The resulting SAM files were converted to BAM files using Samtools (Li et al. 2009). Count files for individual replicates were generated with HTSeq-0.10.0 (Anders et al. 2015) using exon annotations from Pombase (GFF annotations, genome-version ASM294v2; source 'ensembl'). RPKM analysis and calculations of pairwise correlations (Pearson coefficients of 0.978 to 0.987) were performed as described previously (Schwer et al. 2014). Differential gene expression and fold change analysis was performed in DESeq2 (Love et al. 2014). Cut-off for further evaluation was set for genes that had an adjusted p-value (Benjamini-Hochberg corrected) of ≤0.05 and were up or down by at least two-fold in *vtc4Δ* versus wild-type. Genes were further filtered on the following criteria: (i) ≥2-fold up and the average normalized read count for the mutant strain was ≥100; and (ii) ≥2-fold down and the average normalized read count for the wild-type strain was ≥100. Alternatively, a cut-off of at least a four-fold up or down in *vtc4Δ* versus wild-type was set without regard to the normalized read count values, which flagged *SPAC186.04c* as upregulated in *vtc4Δ* cells.

Reverse transcriptase quantitative PCR analysis.

Total RNA was prepared from exponentially growing cells (three independent cultures for each yeast strain analyzed) via the hot phenol method. The RNAs were treated with DNase I, extracted serially with phenol:chloroform and chloroform, and then precipitated with ethanol. The RNAs were resuspended in 10 mM Tris HCl (pH 6.8) and 1 mM EDTA and adjusted to a concentration of 600 ng/μl. Reverse transcription was performed with 2 μg of this RNA template plus oligo(dT)$_{18}$ and random hexamer primers by using the Maxima First Strand cDNA synthesis kit (Thermo Scientific). After cDNA synthesis for 30 min at 55˚C, the reverse transcription reaction mixtures were diluted 10-fold with water. Aliquots (2 μl) were used as templates for gene-specific quantitative PCR (qPCR) reactions directed by the sense and antisense primers listed in Reagents. The qPCR reactions were constituted with the Maxima SYBR Green/ROX master mix (Thermo Scientific) and monitored with an Applied Biosystems QuantStudio 6 Flex Real-Time PCR system. The qPCR reactions were performed in triplicate for each cDNA population. The level of individual cDNAs was calculated relative to that of *act1* cDNA by the comparative Ct method (Schmittgen & Livak 2008). The actin-normalized levels of the four sub-telomeric transcripts in wild-type cells were assigned a value of 1.0 and the mRNA levels in the three *vtc* mutant were then normalized to the wild-type control value.

Data Deposition. The RNA-seq data in this publication have been deposited in NCBI's Gene Expression Omnibus and are accessible through GEO Series accession number GSE213524.

Reagents

Oligonucleotide primers used for qPCR analyses

Gene	Strand	Sequence
act1	Sense	5'–AAGTACCCCATTGAGCACGG
	Antisense	5'–CAGTCAACAAGCAAGGGTGC
SPAC186.04c	Sense	5'–GCGAAGAAAACCCAACAAGC
	Antisense	5'–TCATCGTTTACTCTGATCCGTGA
gdt1 (SPAC186.05c)	Sense	5'–AAATTTTCCCGGGCTTTCAT
	Antisense	5'–TCCGACAATCACCGCTACC
SPAC186.06	Sense	5'–GGGAGTGGAGCTGGATCAGT
	Antisense	5'–CGCCACCAACATGAATATCG
SPAC750.01	Sense	5'–TATTGGGAAGACTGGGTGCTTGAAG
	Antisense	5'–CCAACCAATTCTTCTGACACCCCA

Primers for all genes (except for *act1*) were the same used by Cohen et al. 2018 and 2022.

Fission yeast strains used in this study

Strain	Genotype
BS78	*h+ vtc2Δ::kanMX*
BS128	*h- vtc4Δ::kanMX*
BS623	*h+ vtc4-R262A,R264A::kanMX*

All strains are *leu1-32 ura4-D18 his3-D1* and either *ade6-m216 or ade6-m210*.

References

Anders S, Pyl PT, Huber W. 2015. HTSeq--a Python framework to work with high-throughput sequencing data. Bioinformatics 31: 166-9. PubMed ID: 25260700

Auesukaree C, Homma T, Tochio H, Shirakawa M, Kaneko Y, Harashima S. 2004. Intracellular phosphate serves as a signal for the regulation of the PHO pathway in Saccharomyces cerevisiae. J Biol Chem 279: 17289-94. PubMed ID: 14966138

Azevedo C, Desfougères Y, Jiramongkol Y, Partington H, Trakansuebkul S, Singh J, et al., Saiardi A. 2020. Development of a yeast model to study the contribution of vacuolar polyphosphate metabolism to lysine polyphosphorylation. J Biol Chem 295: 1439-1451. PubMed ID: 31844018

Azevedo C, Livermore T, Saiardi A. 2015. Protein polyphosphorylation of lysine residues by inorganic polyphosphate. Mol Cell 58: 71-82. PubMed ID: 25773596

Azevedo C, Saiardi A. 2014. Functions of inorganic polyphosphates in eukaryotic cells: a coat of many colours. Biochem Soc Trans 42: 98-102. PubMed ID: 24450634

Baker CJ, Smith SA, Morrissey JH. 2019. Polyphosphate in thrombosis, hemostasis, and inflammation. Res Pract Thromb Haemost 3: 18-25. PubMed ID: 30656272

Beaufay F, Amemiya HM, Guan J, Basalla J, Meinen BA, Chen Z, et al., Jakob U. 2021. Polyphosphate drives bacterial heterochromatin formation. Sci Adv 7: eabk0233. PubMed ID: 34936433

Bentley-DeSousa A, Holinier C, Moteshareie H, Tseng YC, Kajjo S, Nwosu C, et al., Downey M. 2018. A Screen for Candidate Targets of Lysine Polyphosphorylation Uncovers a Conserved Network Implicated in Ribosome Biogenesis. Cell Rep 22: 3427-3439. PubMed ID: 29590613

Bondy-Chorney E, Abramchuk I, Nasser R, Holinier C, Denoncourt A, Baijal K, et al., Downey M. 2020. A Broad Response to Intracellular Long-Chain Polyphosphate in Human Cells. Cell Rep 33: 108318. PubMed ID: 33113373

Bowlin MQ, Gray MJ. 2021. Inorganic polyphosphate in host and microbe biology. Trends Microbiol 29: 1013-1023. PubMed ID: 33632603

Cohen A, Habib A, Laor D, Yadav S, Kupiec M, Weisman R. 2018. TOR complex 2 in fission yeast is required for chromatin-mediated gene silencing and assembly of heterochromatic domains at subtelomeres. J Biol Chem 293: 8138-8150. PubMed ID: 29632066

Cohen A, Kupiec M, Weisman R. 2016. Gad8 Protein Is Found in the Nucleus Where It Interacts with the MluI Cell Cycle Box-binding Factor (MBF) Transcriptional Complex to Regulate the Response to DNA Replication Stress. J Biol Chem 291: 9371-81. PubMed ID: 26912660

Cohen A, Pataki E, Kupiec M, Weisman R. 2022. TOR complex 2 contributes to regulation of gene expression via inhibiting Gcn5 recruitment to subtelomeric and DNA replication stress genes. PLoS Genet 18: e1010061. PubMed ID: 35157728

Colinet AS, Sengottaiyan P, Deschamps A, Colsoul ML, Thines L, Demaegd D, et al., Morsomme P. 2016. Yeast Gdt1 is a Golgi-localized calcium transporter required for stress-induced calcium signaling and protein glycosylation. Sci Rep 6: 24282. PubMed ID: 27075443

Desfougères Y, Saiardi A, Azevedo C. 2020. Inorganic polyphosphate in mammals: where's Wally?. Biochemical Society Transactions 48: 95-101. PubMed ID: 32049314

Gerasimaitė R, Mayer A. 2016. Enzymes of yeast polyphosphate metabolism: structure, enzymology and biological roles. Biochem Soc Trans 44: 234-9. PubMed ID: 26862210

Gerasimaite R, Pavlovic I, Capolicchio S, Hofer A, Schmidt A, Jessen HJ, Mayer A. 2017. Inositol Pyrophosphate Specificity of the SPX-Dependent Polyphosphate Polymerase VTC. ACS Chem Biol 12: 648-653. PubMed ID: 28186404

Gerasimaitė R, Sharma S, Desfougères Y, Schmidt A, Mayer A. 2014. Coupled synthesis and translocation restrains polyphosphate to acidocalcisome-like vacuoles and prevents its toxicity. J Cell Sci 127: 5093-104. PubMed ID: 25315834

Gray MJ, Wholey WY, Wagner NO, Cremers CM, Mueller-Schickert A, Hock NT, et al., Jakob U. 2014. Polyphosphate is a primordial chaperone. Mol Cell 53: 689-99. PubMed ID: 24560923

Hothorn M, Neumann H, Lenherr ED, Wehner M, Rybin V, Hassa PO, et al., Mayer A. 2009. Catalytic core of a membrane-associated eukaryotic polyphosphate polymerase. Science 324: 513-6. PubMed ID: 19390046

Kim D, Langmead B, Salzberg SL. 2015. HISAT: a fast spliced aligner with low memory requirements. Nat Methods 12: 357-60. PubMed ID: 25751142

Kornberg A, Rao NN, Ault-Riché D. 1999. Inorganic polyphosphate: a molecule of many functions. Annu Rev Biochem 68: 89-125. PubMed ID: 10872445

Laribee RN, Weisman R. 2020. Nuclear Functions of TOR: Impact on Transcription and the Epigenome. Genes (Basel) 11: . PubMed ID: 32532005

Li H, Handsaker B, Wysoker A, Fennell T, Ruan J, Homer N, et al., 1000 Genome Project Data Processing Subgroup. 2009. The Sequence Alignment/Map format and SAMtools. Bioinformatics 25: 2078-9. PubMed ID: 19505943

Liger D, Quevillon-Cheruel S, Sorel I, Bremang M, Blondeau K, Aboulfath I, et al., Leulliot N. 2005. Crystal structure of YHI9, the yeast member of the phenazine biosynthesis PhzF enzyme superfamily. Proteins 60: 778-86. PubMed ID: 16021630

Lima CD, Wang LK, Shuman S. 1999. Structure and mechanism of yeast RNA triphosphatase: an essential component of the mRNA capping apparatus. Cell 99: 533-43. PubMed ID: 10589681

Love MI, Huber W, Anders S. 2014. Moderated estimation of fold change and dispersion for RNA-seq data with DESeq2. Genome Biol 15: 550. PubMed ID: 25516281

Martinez J, Truffault V, Hothorn M. 2015. Structural Determinants for Substrate Binding and Catalysis in Triphosphate Tunnel Metalloenzymes. J Biol Chem 290: 23348-60. PubMed ID: 26221030

Pascual-Ortiz M, Walla E, Fleig U, Saiardi A. 2021. The PPIP5K Family Member Asp1 Controls Inorganic Polyphosphate Metabolism in S. pombe. J Fungi (Basel) 7: 626 . PubMed ID: 34436165

Schmittgen TD, Livak KJ. 2008. Analyzing real-time PCR data by the comparative C(T) method. Nat Protoc 3: 1101-8. PubMed ID: 18546601

Schwer B, Bitton DA, Sanchez AM, Bähler J, Shuman S. 2014. Individual letters of the RNA polymerase II CTD code govern distinct gene expression programs in fission yeast. Proc Natl Acad Sci U S A 111: 4185-90. PubMed ID: 24591591

Schwer B, Garg A, Sanchez AM, Bernstein MA, Benjamin B, Shuman S. 2022. Cleavage-Polyadenylation Factor Cft1 and SPX Domain Proteins Are Agents of Inositol Pyrophosphate Toxicosis in Fission Yeast. mBio 13: e0347621. PubMed ID: 35012333

Wild R, Gerasimaite R, Jung JY, Truffault V, Pavlovic I, Schmidt A, et al., Mayer A. 2016. Control of eukaryotic phosphate homeostasis by inositol polyphosphate sensor domains. Science 352: 986-90. PubMed ID: 27080106

Citation: Sanchez, AM; Garg, A; Schwer, B; Shuman, S (2023). Inorganic polyphosphate abets silencing of a sub-telomeric gene cluster in fission yeast. microPublication Biology. 10.17912/micropub.biology.000744